

A recent and comprehensive compilation of the hydrogen bonding in amino acids, peptides, and related molecules⁵² shows that N-H...X⁻ (X = Cl and Br) bonds are appreciably longer and therefore weaker than hydrogen bonds to other likely acceptors such as acetate, phosphate, and sulfate oxygen atoms. No instances of N-H...F⁻ systems appear to have been subjected to crystal structure determination.

From our calculations and studies it seems certain that the F⁻ ion competes successfully for the N-H bond in amide systems. Other N-H bonds could also be affected. Considering the prevalence of hydrogen bonding involving N-H in biological systems, including DNA, it may well be important to avoid undue exposure in high concentrations of fluoride ion, which may be able to disrupt them.

The profound biological effects that are being linked to the simple fluoride ion such as genetic damage, birth defects, allergy

responses, and cancer⁵³ are difficult to explain as arising from the chemistry of this ion, which in aqueous solution is stable and not active in bond-forming or bond-breaking reactions, being a very weak nucleophile. We believe that we have found, in its strong hydrogen bonding potential toward the NH group of amides and related biomolecules, an explanation of how this reputedly inert ion could disrupt key sites in biological systems. By the same token it may also explain why fluoride is an essential element in low concentrations, use being made of the N-H-F⁻ hydrogen bond as an intermediate step in reactions involving amides.

Acknowledgment. The authors wish to thank NATO for a travel grant (J.E. and J.M.M.) and the Science Research Council of Great Britain for a maintenance grant (D.J.J.).

(52) S. N. Vinogradov, *Int. J. Peptide Protein Res.*, **14**, 281 (1979).

(53) G. L. Waldbott, A. W. Burgstahler, and H. L. McKinney, "Fluoridation: the Great Dilemma", Coronado Press, Lawrence, Kansas, 1978.

NMR Study of Molecular Reorientation under Fivefold Symmetry — Solid Permethylferrocene[†]

D. E. Wemmer, D. J. Ruben, and A. Pines*

Contribution from the Materials and Molecular Research Division, Lawrence Berkeley Laboratory, University of California, Berkeley, California 94720. Received March 24, 1980

Abstract: The ring reorientation in permethylferrocene has been studied by using high-resolution solid-state ¹³C NMR. The constraints which symmetry places upon the number and types of motional parameters which may be determined from the NMR spectrum are discussed. From comparison of the experimental line shapes in the slow reorientation temperature range with theoretical models for random rotations and symmetry-related jumps, it is concluded that the reorientation occurs as jumps between symmetry-related orientations with jumps of $2\pi/5$ highly favored over $4\pi/5$. The activation energy derived for the jump process is 13.5 kJ/mol.

1. Introduction

NMR has long played an important role in the study of molecular motion in the solid state.^{1,2} However, most of the experiments to date have been low resolution in nature, observation of narrowing of dipolar broadened lines or measurement of relaxation times T_1 and $T_{1\rho}$, and thus are limited in ability to distinguish among different types of molecular motion. Recent advances in solid state NMR techniques³ have made available high-resolution line shapes for chemical shielding and thus the possibility for much more detailed analysis of molecular motions in the solid state. Early studies of this type were made in cases for which the motion is of sufficiently high symmetry to reduce the powder line shape to a single sharp line.^{4,5,7} In such cases it is possible to distinguish experimentally between models of rotational diffusion and jumps between symmetry-related orientations, in spite of the fact that the rapid motion line shapes are the same. Theoretical⁶ and experimental^{7,8} work has shown that similarly detailed information may also be obtained in cases where the motion is of lower symmetry.

In this paper we present an analysis of ring rotation in permethylferrocene, using the high-resolution approach. This case is of particular interest because of the C_5 symmetry, which requires two parameters, corresponding to jumps of $2\pi/5$ and $4\pi/5$ for a jump model. Though it may be possible to distinguish the relative probability of such jumps by using neutron scattering,⁹ no such analysis has yet been successfully completed. However,

since the different types of jumps lead to different kinds of averaging in the ¹³C line shapes, the relative probability may be ascertained through analysis of line shapes obtained in the slow-exchange temperature region.

2. ¹³C Line Shapes for Limiting Cases of Motion

In rigid powder solids, high-resolution ¹³C spectra may be completely characterized by one, or more possibly overlapping chemical shielding tensors. If a carbon is at a site of low symmetry, then its line shape is the well-known tensor powder pattern calculated first by Bloembergen and Rowland.¹⁰ If some rapid molecular motion occurs (rapid meaning that the correlation time is much shorter than the inverse of the spectral width involved), then this tensor must be averaged over the motion with an appropriate angular weighing function. If the motion is isotropic, as in plastic phases, then the chemical shielding tensors are reduced to just their trace. If the motion is a uniform uniaxial rotation,

(1) H. S. Gutowsky and G. E. Pake, *J. Chem. Phys.*, **18**, 162 (1950).

(2) E. R. Andrew, *J. Chem. Phys.*, **18**, 607 (1950).

(3) M. Mehring, "NMR: Basic Principles and Progress", Vol. 11, Springer Verlag, Heidelberg, 1976.

(4) H. W. Spiess, *Chem. Phys.*, **6**, 217 (1974).

(5) H. W. Spiess, R. Grosescu, and U. Haebleren, *Chem. Phys.*, **6**, 226 (1974).

(6) A. Baram, Z. Luz, and S. Alexander, *J. Chem. Phys.*, **64**, 4321 (1976).

(7) D. Wemmer, Ph.D. Thesis, University of California, Berkeley, 1979.

(8) D. Wemmer, D. J. Ruben, and A. Pines, to be submitted for publication.

(9) J. Tomkinson, private communication.

(10) N. Bloembergen and T. J. Rowland, *Acta Metallurgica*, **1**, 731 (1955).

[†]Taken in part from the Ph.D. Thesis of D. E. Wemmer, Lawrence Berkeley Laboratory Report No. LBL-8042, 1978.

then the shielding tensors will be only partially averaged and give then the axially symmetric pattern also described by Bloembergen and Rowland. As has been described,^{11,12} a knowledge of the unaveraged and averaged tensors suffices to give the direction of the rotation axis relative to the shielding tensor axis system. Since it is often possible to assign at least some tensor element directions through considerations of molecular symmetry and through use of known single-crystal data, the axialization can provide detailed geometrical information about the motion which is not available from wide-line proton NMR studies. However, the line shape can provide still more detailed information in some cases.

3. Models for Motion in the Slow-Exchange Region

To describe the line shapes for ¹³C in the presence of rapid molecular motion, the rigid shielding tensors are replaced by averaged tensors, with the averaging used determined by the nature of the motion. However, when the molecular motion occurs at a rate comparable to the spread of frequencies involved, the ¹³C line shapes may no longer be described by a tensor and depend very much on the details of the molecular reorientation process.

Two types of models have been used for description of line shapes in the presence of molecular motions; we will term these random rotations and symmetry-related jumps. In both types of model motion either may occur freely in three dimensions or may be restricted to be about a single axis due to geometrical constraints within the crystal. In the random rotations model there are then no further restrictions; however, different limits in the size of angular jumps allowed exist. If jumps occur only through very small angles, then this is the usual rotational Brownian motion. For jumps through large angles, one may consider the initial and final orientations to be totally uncorrelated. Though still a rotational diffusion model, this hard collision limit leads to a very different orientational correlation function¹⁵ and may give rise to different NMR line shapes. In either of these limits, it is assumed that only one time constant, corresponding to the average time between jumps, is necessary to fully describe the motion. In the symmetry-related jumps model only certain orientations of the molecule, determined by a combination of molecular geometry and hindering potential, are allowed, and jumps may occur only between these orientations. One then has as parameters the rate of jumps between the various pairs of orientations, though as discussed below for reasons of symmetry some of these may be equal or indistinguishable for the NMR experiment.

4. Symmetry Arguments in Line Shape Calculations

Baram, Luz, and Alexander¹³ have developed a series expansion approach for the calculation of line shapes in the slow-exchange regime. Though applicable for both models, symmetry plays an important role in simplifying the calculations for the symmetry-related jumps model, and we may follow their arguments, based on Rigny,¹⁹ for this work. We begin with the well-known exchange equations for magnetization g including the jumps between sites:

$$\alpha_j g_j + \sum_k W_{jk}(g_k - g_j) = P_j \quad (1)$$

where the subscripts refer to possible sites of a spin for a given

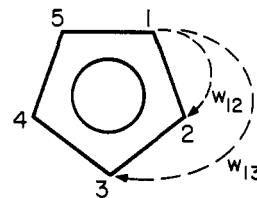


Figure 1. Schematic representation of a five-member ring in the permethylferrocene molecule with the two distinguishable types of jumps which must be considered in the symmetry-related jumps model.

molecular orientation and $\alpha_j = i(\omega - \omega_j) - T_{2j}^{-1}$, ω_j is the Larmor frequency in the j th site, T_{2j} is the transverse relaxation time in the j th site, and W_{jk} is the rate of transitions from j to k . If G is the symmetry group for the allowed positions of a spin, then the g_j provide a basis for a reducible representation of G . Each W_{jk} may be associated with some group element R in G , in particular with R such that $Rg_j = g_k$. The elements R are divided in G into conjugate classes, and since each element of a conjugate class achieves the same exchange of magnetization, their individual rates are not distinguishable for the NMR experiment. We may then assign a single rate W_c for the class, which is the sum of the individual rates for elements in that class. We may rewrite (1)

$$\alpha_j g_j + \sum_c W_c \sum_{\gamma \in c} (R_\gamma - 1) g_j = P_j \quad (2)$$

The g_j may also be expanded in basis functions $g_{\gamma\mu}$ of G

$$g_j = \sum_\gamma \sum_\mu a_{\gamma\mu} g_{\gamma\mu} = \sum_\gamma g_{j\gamma} \quad (3)$$

where λ labels the representation of G and μ the row in a multidimensional representation. We may use the group theoretical result

$$\sum_{\gamma \in c} R_\gamma g_{\gamma\mu} = N_c (\chi_c^\lambda / \nu_\lambda) g_{\gamma\mu} \quad (4)$$

where χ_c^λ is the character of the class in the λ representation, N_c is the number of elements in the class, and ν_λ is the dimension, to rewrite the sum in (2)

$$\sum_c W_c \sum_{\gamma \in c} (R_\gamma - 1) g_{\gamma\mu} = - \sum_c W_c N_c \sum_\gamma (1 - (\chi_c^\lambda / \nu_\lambda)) g_{j\gamma} = - \sum_\gamma W_\gamma g_{j\gamma} \quad (5)$$

where we define the rate for the representation as

$$W_\gamma = \sum_c W_c N_c (1 - (\chi_c^\lambda / \nu_\lambda)) \quad (6)$$

Thus we have replaced the summation over individual rates for exchange between sites with rates for the irreducible representations of the symmetry group for the exchange problem. However, the symmetry can be used further to simplify analysis. Among the elements of G there will be a subgroup S whose operations leave g_j unchanged. Since we wish to calculate the total magnetization, proportional to g_{A1} , we may restrict the summation of λ in (5) to those representations mixed with $A1$. These "relevant" irreducible representations of G are those which when being taken as reducible representations of S contain the totally symmetric representation of S . That is if

$$N_\lambda = \sum_{ces} N_c \chi_c^\lambda \chi_c^{A1}$$

is not zero the λ representation is relevant and must be included in the summation. Noting that $W_{A1} = 0$ in every case, it is clear that we will have one independent motional parameter for each relevant representation beyond $A1$.

5. The Case of C_5 Symmetry

For permethylferrocene we may consider the symmetry group G of the motion to be D_5 , assuming there is no cooperative motion of the rings, an assumption born out by experimental results below. For the chemical shielding tensor the subgroup S is C_2 , and the relevant representations of G are A_1 , E_1 , and E_2 . Thus two in-

(11) A. Pines and D. Wemmer, submitted for publication in *J. Am. Chem. Soc.*

(12) M. Mehring, R. G. Griffin, and J. S. Waugh, *J. Chem. Phys.*, **55**, 746 (1971).

(13) S. Alexander, A. Baram, and Z. Luz, *Mol. Phys.*, **27**, 441 (1974).

(14) A. Abragam, "Principles of Nuclear Magnetism", Oxford University Press, London, 1961.

(15) R. G. Gordon, *J. Chem. Phys.*, **44**, 1830 (1965).

(16) A. Pines, M. G. Gibby, and J. S. Waugh, *J. Chem. Phys.*, **59**, 569 (1973).

(17) A. Pines, Lawrence Berkeley Laboratory, Material and Molecular Research Division Annual Report, 1976, LBL-6016.

(18) C. H. Holm and J. A. Ibers, *J. Chem. Phys.*, **30**, 885 (1959); L. N. Mulay and A. Attalla, *J. Am. Chem. Soc.*, **85**, 702 (1963); M. K. Makova, E. V. Leonova, Yu S. Karimov, and N. S. Kochetkova, *J. Organomet. Chem.*, **55**, 185 (1973).

(19) P. Rigny, *Physica*, **59**, 707 (1972).

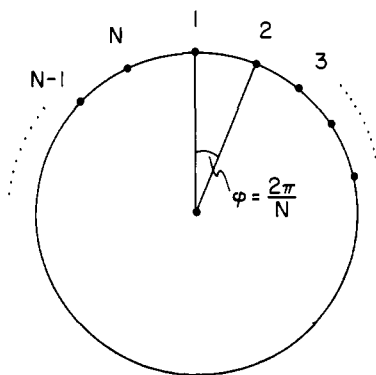


Figure 2. Extension of the symmetry-related jumps model to a large number of sites evenly spaced on a ring provides a good approximation to the hard collision limit of the random jumps model. This becomes exact as N becomes very large.

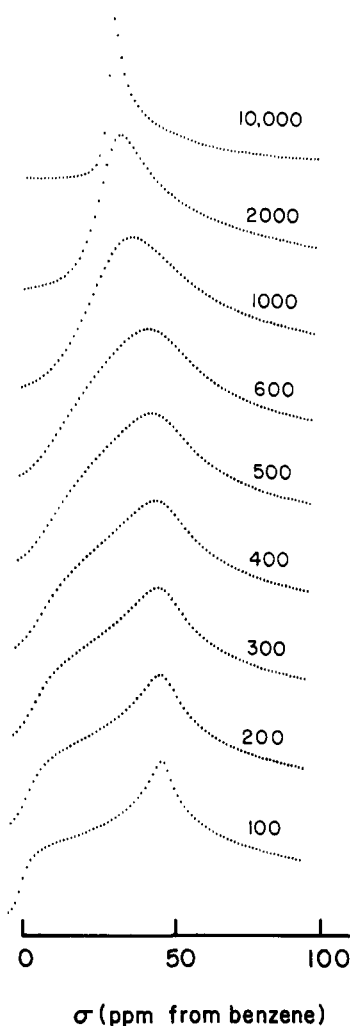


Figure 3. Line shapes are shown for the hard collision random jumps models, calculated with the approximation described, $N = 24$ in Figure 2, for a number of different jump rates.

dependent parameters are necessary for description of the motion. This is quite easy to understand from a physical viewpoint. Figure 1 shows a five-carbon ring, which we may take to have a ^{13}C at position 1. A jump may take the carbon to any site; however, since jumps of $2\pi/5$ and $-8\pi/5$ (and similarly $4\pi/5$ and $-6\pi/5$) belong to the same class of G and hence leave the carbon in the same final position, the rates of such jumps can not be independently determined. We then may take as parameters the rate of jumps to neighboring positions W_{12} and to next neighbor positions W_{13} . Alternately one may use the more fundamental rates for the representations, $W_{E1} = 1.38W_{12} + 3.62W_{13}$ and $W_{E2} = 3.62W_{12}$

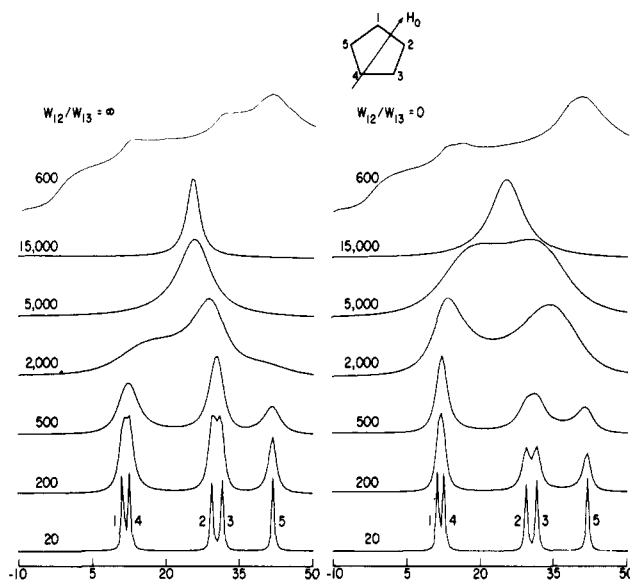


Figure 4. Calculated single-crystal spectra for one particular molecular orientation, together with powder line shapes (at an intermediate jump rate) are shown in the two limits $W_{12} \gg W_{13}$ and $W_{12} \ll W_{13}$. It is clear that the individual spectra are different for the two models and that they contribute to different features in the powder line shapes, making them experimentally distinguishable.

+ $1.38W_{13}$. Since the coupling observed, chemical shielding, is independent of the relative orientations of the two rings, it is impossible to obtain any information about their relative motion.

6. Calculation of Line Shapes for Slow Exchange

The expansion method for calculation of line shapes developed by Baram et al.^{6,13} may be applied to both the random jumps and symmetry-related jumps model. However, for computation in the symmetry-related jumps case with more than one parameter it is not advantageous, and we have used instead a straightforward numerical approach, applying the formalism of chemical exchange. We will show that this method may also be used to approximate the rotational random jumps model.

For a particular molecular orientation, there will be a number of sites which a spin may occupy, each with its particular resonance frequency ω_j , determined by chemical shielding. For known molecular orientation and chemical shielding tensor the site frequencies are easily calculated. The jumping rotation of the ring serves to exchange the spin among the different allowed sites, with the rates, $1/\tau_{jk}$, for jumps from site j to site k specified according to the symmetry and particular model at hand. Since the sites are positions related by molecular symmetry, the populations of sites must be equal. One may then write the exchange equations in matrix form¹⁴

$$\mathbf{A}\mathbf{g} = -i\omega_1 M_0 \mathbf{l} \quad (7)$$

where g_j is the magnetization of site j , \mathbf{A} is the coupling matrix described below, ω_1 is the radio frequency field strength, and M_0 is the equilibrium magnetization. The diagonal elements of \mathbf{A} contain the site information

$$A_{jj} = i(\omega - \omega_j) - \frac{1}{T_2} - \frac{1}{\tau_j} \quad (8)$$

where T_2 is the transverse relaxation time and $\tau_j^{-1} = \sum_{k \neq j} \tau_{kj}^{-1}$. The off-diagonal elements are the exchange rates τ_{jk}^{-1} . We wish to calculate the absorption line shape, proportional to the imaginary part of the total magnetization $g(\omega) = \sum_j g_j$. We may formally solve (7) for \mathbf{g} as

$$\mathbf{g} = -i\omega_1 M_0 \mathbf{A}^{-1} \mathbf{l} \quad (9)$$

or in terms of elements of \mathbf{A}^{-1}

$$g(\omega) = \text{Im}(\sum_j -i\omega_1 M_0 \sum_k A_{jk}^{-1}) = -\omega_1 M_0 \text{Re}(\sum_{jk} A_{jk}^{-1}) \quad (10)$$

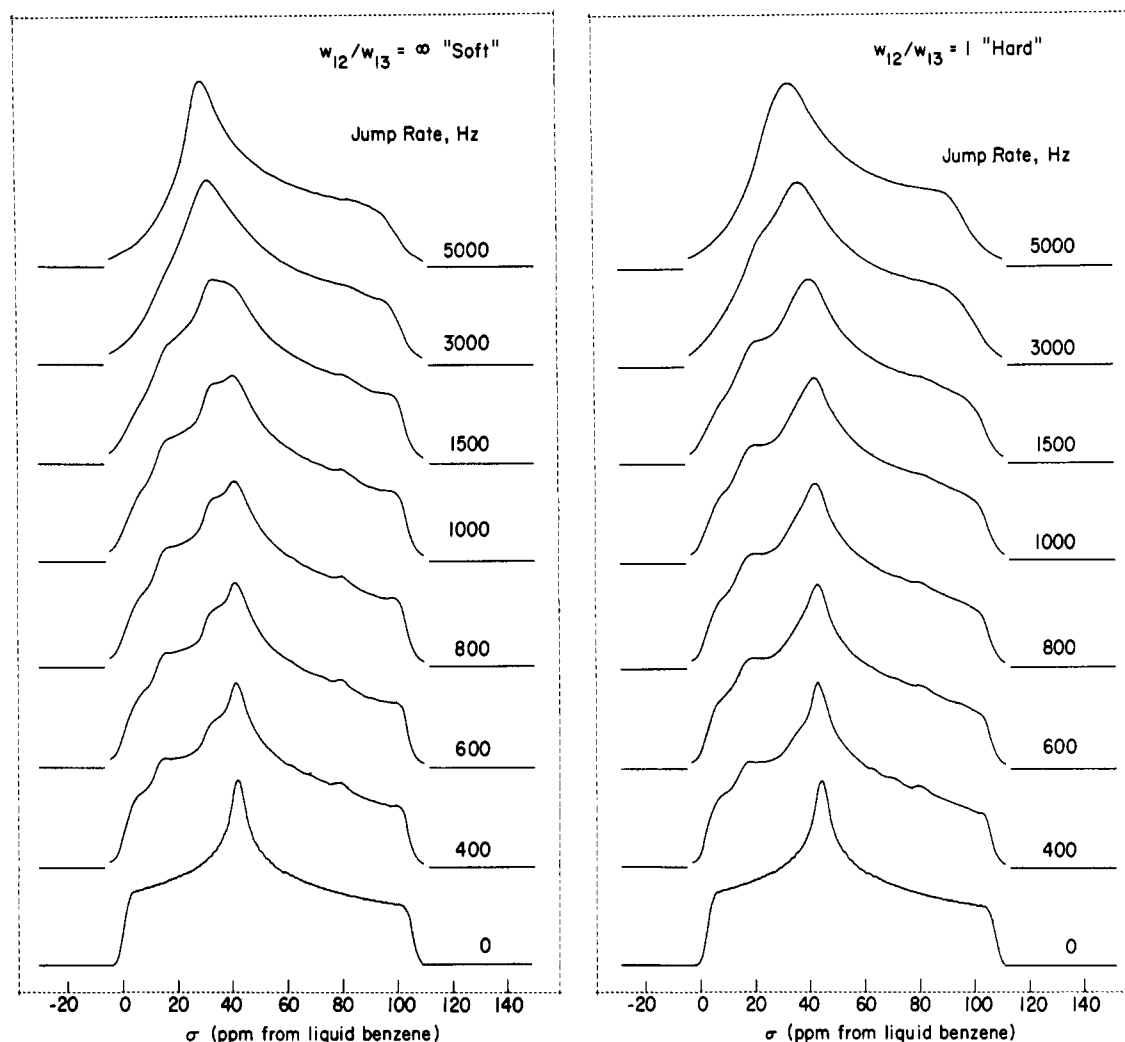


Figure 5. Complete powder line shapes are shown for the two physically reasonable models $W_{12} \gg W_{13}$ and $W_{12} = W_{13}$, at several total jump rates. The extra "bumps" in these spectra relative to random jumps are clearly evident in the downfield region.

One must calculate A^{-1} for each value of ω desired for each molecular orientation. However, the complete diagonalization or inversion need not be repeated for each different ω , since the transformation matrix to diagonalize does not change with ω , which appears only on the diagonal.¹⁵

Since g is a function of the molecular orientation Ω , as well as ω , to obtain the powder line shape we must integrate $g(\omega, \Omega)$ with appropriate weighting

$$I(\omega) = \int_{\Omega} g(\omega, \Omega) d\Omega \quad (11)$$

This is easily achieved through use of a $\sin \theta$ weighting in the sampling of the various orientations $\Omega = (\phi, \theta, \gamma)$ which are summed to give the powder spectrum. It is worth noting that due to high molecular symmetry and the symmetry of the chemical shielding it is often possible to greatly reduce the range of angles which must be integrated. One must be certain to sample densely enough in both frequency and orientation to prevent artifactual features in the line shapes. Satisfactory parameters are easily found by increasing the number of points sampled until no further changes occur in the calculated spectra. We found 100 frequency points for each of ~ 2500 orientations to be sufficient.

The line shapes for rotational random jumps in the hard-exchange limit are obtained with the same method except that the number of allowed orientations is taken to be a large number (24 in the present case), with an equal probability for jumps between any pair. This is shown schematically in Figure 2. As is discussed elsewhere, diagonalization of the exchange matrix in this case can be done analytically, making the calculation much faster and simpler. The line shapes thus obtained agree very well with those

obtained by Baram et al. using expansion methods.

7. Significant Features of the Slow-Exchange Line Shapes

In order to experimentally distinguish among the possible models for rotational motion, the different models must lead to significantly different line shapes. We will see that this is so for cases of high symmetry (such as D_5) due to the fundamentally different averaging processes which occur in the different models.

When rotational random jumps occur, the spin is exchanged among sites with a continuous range of chemical shifts. For slow to intermediate exchange rates this leads to a broad line for each molecular orientation and hence a powder line shape which broadens with increasing exchange rates, without any particular features. Eventually for high exchange rates each orientation contributes a sharp line at the appropriately weighted average position, and the powder line shape converges to that of the appropriately averaged tensor. Line shapes are shown at a variety of exchange rates in Figure 3, for the hard collision, 24-site approximation calculated by using our method. The features do not differ significantly from those obtained by other workers using other methods. These also differ very little from the weak collision rotational diffusion limit.

In the symmetry-related jumps model, the averaging process is quite different. Each nonexchanging molecular orientation gives a spectrum of at most five lines. The jumping process serves to exchange magnetization among these five frequencies in a manner determined by the parameters W_{12} and W_{13} . It is more convenient to use as working parameters the total rate of jumps $W_{12} + W_{13}$ and the ratio of the two types W_{12}/W_{13} . The averaging of the

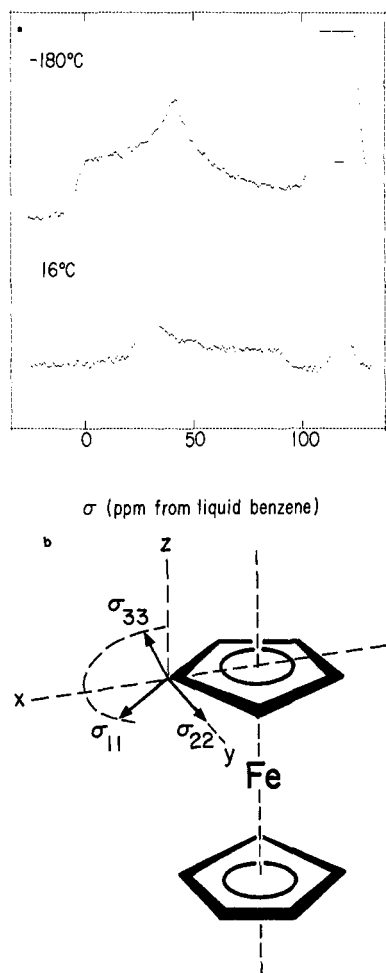


Figure 6. (a) High- and low-temperature ^{13}C spectra of permethylferrocene showing ring carbon and methyl carbon (truncated) peaks. (b) The probable shielding tensor orientation for the ring carbons is also shown schematically.

five lines is very different from the random jumps model when two of the lines start out close together. If the jumping process exchanges magnetization directly between these two lines, then they will be averaged more rapidly than the other lines and may lead to a significant feature even in the powder line shape. Such averaging leading to features has been predicted and observed both in cases of three-dimensional jumps and for planar rotations and jumps. An example of the averaging is shown in Figure 4 for one particular orientation. As can be seen, the line shapes for such an orientation differ considerably in the two limits $W_{12} \gg W_{13}$ and $W_{12} \ll W_{13}$. The contributions of such orientations to the powder line shape are manifested as extra "bumps" in the line shape. Complete calculated line shapes for a number of exchange rates are shown in Figure 5 for two physically reasonable limits: soft jumps $W_{12} \gg W_{13}$ and hard jumps $W_{12} = W_{13}$. Although they are generally similar, they differ considerably in the region near 30 ppm. This difference stems from which sites have magnetization directly exchanged as demonstrated in Figure 4.

8. Experiments

Experimental ^{13}C spectra were obtained by using the cross-polarization approach,¹⁶ on a home built spectrometer¹⁴ operating at a proton frequency of 185 MHz and carbon frequency of 46.5 MHz. The sample of permethylferrocene (300 mg of powder compressed into a 6-mm diameter pellet) was prepared in the laboratory of and given to us by Professor George Whitesides of MIT. It was estimated to be greater than 98% purity. The sample temperature was maintained constant to ± 0.2 °C through a flow of cold nitrogen gas generated by boiling liquid nitrogen, together

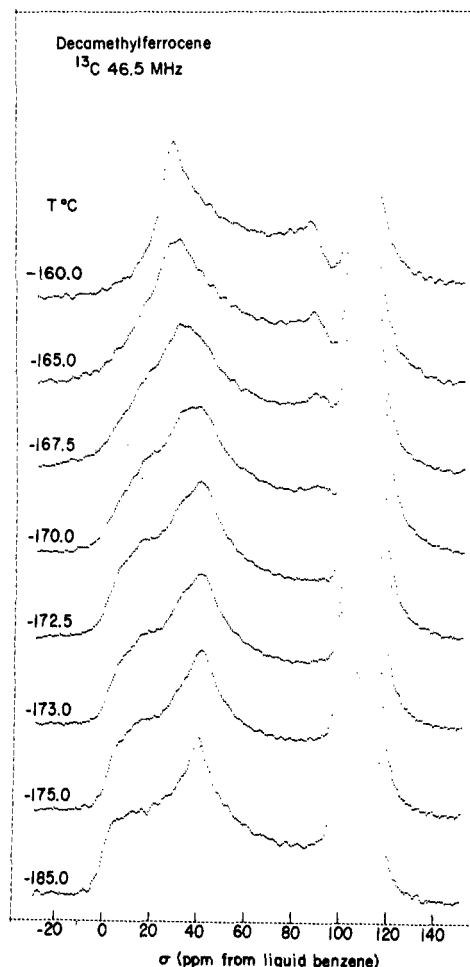


Figure 7. The temperature dependence of the carbon line shape of permethylferrocene is shown. The features in the low-field region clearly demonstrate that the symmetry-related jumps model must be used for analysis.

with a digitally controlled feedback heating coil fitted in the gas stream near the sample. The absolute temperature was determined by a thermocouple indicator to an estimated absolute accuracy of ± 1 °C. At each temperature the cross-polarization parameters, contact time, and recycle delay were empirically adjusted for maximum signal. Rotating fields of about 10 G for protons and 40 G for carbon were used. The contact times varied from 0.5 to 5 ms. Several hundred free induction decays were averaged at each temperature before Fourier transformation to give the absorption spectra.

The high- and low-temperature line shapes for permethylferrocene are shown in Figure 6. The low-temperature line shape is characterized by a ring-shielding tensor with elements $\sigma_{11} = 1.0$ ppm, $\sigma_{22} = 42.5$ ppm, and $\sigma_{33} = 105.1$ ppm (all tensor elements reported relative to an external standard of liquid benzene and are estimated at ± 1 ppm accuracy). The second peak on the upfield side, which is truncated in these spectra, comes from the methyl carbons and is not of interest here. The room-temperature spectrum shows an axially symmetric shielding tensor with $\sigma_1 = 27.3$ ppm and $\sigma_{11} = 94.0$ ppm, indicating a rapid uniaxial motion, as expected. The determination of the tensor orientation and comparison with other organometallics are reported in more detail elsewhere.¹¹ The shift upon rotation of the upfield tensor element indicates that the rotation axis does not correspond to a principle direction for the shielding tensor such as has been observed for hexamethylbenzene.^{7,8,16} If one assumes motion to be about the C_5 axis of the molecule, then one may calculate that the σ_{33} elements direction is rotated 19° from the rotation axis.¹¹

The temperature dependence of the line shape is shown for the interesting temperature region in Figure 7. From the structure immediately evident in the line shapes it is clear that the sym-

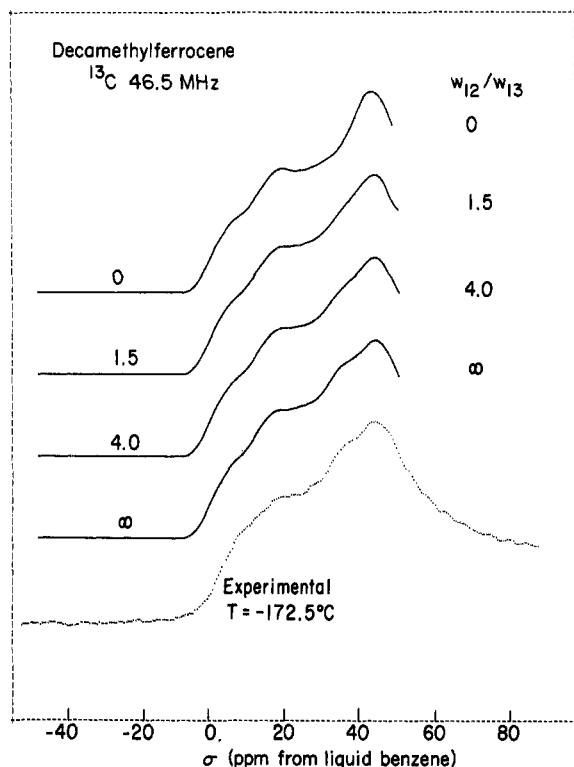


Figure 8. The experimental line shape for the ring carbon is compared to theoretical line shapes for one total jump rate (800 Hz) and several W_{12}/W_{13} ratios. The feature near ~ 35 ppm is most sensitive to this ratio, and clearly a large W_{12}/W_{13} ratio agrees best with the experiment.

metry-related jumps model must be used for analysis, as has been true in earlier studies.⁵⁻⁸ The rate of jumps may be determined through comparison of the features of the experimental line shapes with the theoretical ones in Figure 5. To further evaluate the parameter W_{12}/W_{13} we examine the line shape at -172.5 °C in more detail. Figure 8 shows the downfield region of this spectrum together with calculated line shapes for one total jump rate and a number of values of W_{12}/W_{13} . From the intensity of the feature near -35 ppm, it is clear that only a large value of W_{12}/W_{13} will correctly reproduce the experimental spectrum. However, since the line shape rapidly approaches its final shape for large values of this ratio, we can only estimate the $W_{12}/W_{13} \geq 10$, that is to say jumps of $2\pi/5$ are strongly favored over jumps of $4\pi/5$. Since this is true, it is clear that we may view the total jump rate as the rate of jumps of $2\pi/5$ and ignore those of larger angle com-

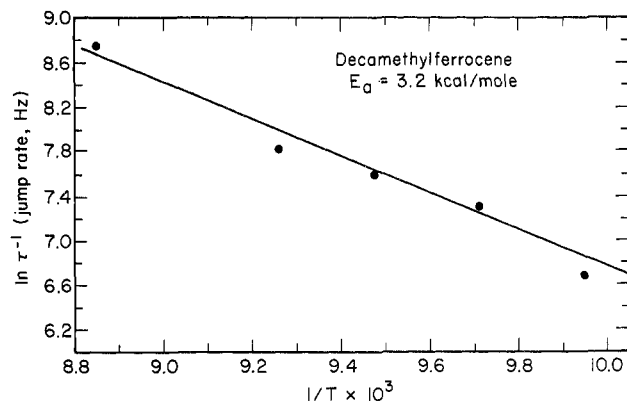


Figure 9. An activation energy plot for permethylferrocene is shown. Rates were determined by comparison of features in experimental and theoretical spectra.

pletely. In addition, the strong features evident for the $2\pi/5$ jumps case rule out the possibility of cooperative rotation of the two rings for an effective D_{10} symmetry, since such a model would result in weaker features (closer to the random model) in other positions.

By comparison of the theoretical and experimental spectra the jump rate as a function of temperature may be estimated, and an Arrhenius plot (Figure 9) made to obtain the activation energy for the jumping process. For permethylferrocene this analysis gives 13.5 kJ/mol, somewhat higher than the ~ 8.4 kJ/mol measured for ferrocene¹⁸ but quite reasonable for a permethyl derivative.

9. Conclusions

To our knowledge these measurements represent the first analysis of molecular reorientation in a solid for which more than one correlation time for planar jumps can be distinguished. The much higher probability for $2\pi/5$ jumps in this C_5 symmetry case must stem from a high probability for deactivational collisions of activated rotating molecules. The line shapes analysis demonstrates that the very high sensitivity of NMR chemical exchange line shapes to the microscopic details of molecular reorientation can be exploited in the solid state. It is clear that this approach is not limited to polycrystalline samples but may equally well be applied in single crystals, molecules adsorbed on surfaces, and other partially ordered systems.

Acknowledgment. We would like to thank Professor G. Whitesides for giving us the sample of permethylferrocene. This work was supported by the Division of Materials Sciences, Office of Basic Energy Sciences, U.S. Department of Energy, under Contract No. W-7405-Eng-48.